Short Communication

Interface Modification by Cs$_2$CO$_3$ Buffer Layer in Electroluminescent Quantum Dot Light-Emitting Diodes with Metal-Oxide Carrier Transport Layers

Chun-Yuan Huang[1,] and Ying-Chih Chen[2]*

[1]Department of Applied Science, National Taitung University, Taitung 950, Taiwan
[2]Institute of Microelectronics, Advanced Optoelectronic Technology Center, and LED Lighting and Research Center, National Cheng Kung University, Tainan 701, Taiwan
[*]E-mail: Laputa@nttu.edu.tw

In this article, the quantum dot (QD) light-emitting diodes (QDLEDs) with ZnO electron transport layer (ETL) and MoO$_3$ hole transport layer (HTL) were demonstrated. With adequate mixing of 0.1 M zinc acetate dihydrate and monoethanolamine (MEA) in ethyl alcohol, the ZnO ETL was readily fabricated on indium tin oxide (ITO)/glass substrates by sol-gel method. To achieve balanced electron and hole injection, Cs$_2$CO$_3$ and 4,4'-di(N-carbazolyl)biphenyl (CBP) layers were inserted prior to the deposition of QD and MoO$_3$ layers, respectively. Our device structure can be simply depicted as ITO/ZnO/Cs$_2$CO$_3$/QD/CBP/MoO$_3$/Au. It was found that the Cs$_2$CO$_3$ buffer layer played an important role to facilitate radiative recombination and reduce the leakage current due to the poor quality of sol-gel fabricated ZnO thin films. The analysis of surface morphology of Cs$_2$CO$_3$ layers showed that ZnO/QD interface can be effectively formed for electron injection only when the Cs$_2$CO$_3$ layer was annealed properly. With our demonstration, QDLEDs with ZnO ETL and MoO$_3$ HTL can be a promising device structure for realizing QDLED's commercial application.

1. INTRODUCTION

In recent two decades, the chemically-synthesized colloidal semiconductor quantum dots (QDs), or nanocrystals, have attracted considerable attention for their biomedical, electronic, and optoelectronic applications [1-4]. Their foremost advantages include high chemical and optical stabilities, easy tuning of the saturated color emission across the visible-NIR range, and easy processability in hybridizing with organic and inorganic materials [2-6]. For the most used CdSe/ZnS

core/shell QDs, three primary emission colors can be obtained by simply adjusting core size. So far, QDs with high luminescence quantum yield near unity (100%) have been reported [6,7], indicating the QD is no longer just a theoretically ideal material. Among the applications, electroluminescent QD-light-emitting diodes (QDLEDs) were proposed as the next generation display technology to replace liquid crystal display (LCD) and upcoming organic light-emitting diodes (OLEDs). With similar device physics and operation mechanism, the development of QDLEDs frequently learned from the experience in developing OLEDs, such as the improvement of device architecture and processing, and the use of metal oxides for carrier transport [8-10].

Numerous metal oxides have been reported to facilitate carrier transport in OLEDs, including NiO, WO_3, and MoO_3 for hole transport and TiO_2, ZrO_2, ZnO for electron injection [10-12], basically due to their high ionization energy or low electron affinity to reduce the potential barrier when these ceramics were in contact with organic emissive layers. Though these inorganic metal oxide films can be deposited by physical and chemical processes [10-12], sol-gel fabricated metal oxides seems a more suitable candidate for the practical demands of low-cost and mass-production. Furthermore, alkali metal compounds such as Cs_2CO_3, LiF, and CsF were known to reduce the operating voltage, modify the energy band, and prevent cathode-induced luminescence quenching [13]. The combination of metal oxides and alkali metal compounds has significantly improve the performance of OLEDs, meanwhile similar revolution is taking place on the design of QDLEDs [9,14].

Based on previous studies [8,15-17], QDLEDs with CdSe/ZnS core/shell QDs, poly(3,4,ethylenedioxythiophene)-poly (styrenesulfonate) (PEDOT-PSS) and poly(N,N'-bis (4-butylphenyl)-N,N'-bis(phenyl) benzidine) (poly-TPD) hole transport layer (HTL) suffered large injection barrier and low device reliability. Consequently, device characteristics such as operation voltage and luminance efficiency could be deteriorated. In this article, we demonstrated the electroluminescent QDLEDs with ZnO and MoO_3 layers for electron and hole transport, respectively. Besides the well-known barrier modification, we found that the Cs_2CO_3 buffer layer and its annealing treatment have played important roles to facilitate radiative recombination and reduce the leakage current due to the extensively distributed voids, pores and grain boundaries in sol-gel fabricated ZnO thin films. Via inserting an annealed Cs_2CO_3 buffer layer with proper thickness, red-emitting QDLEDs with low luminance turn-on voltage of 4.1 V and luminance larger than 150 cd/m^2 can be obtained.

2. EXPERIMENTAL DETAILS

In device fabrication, inverted structure with indium tin oxide (ITO) acting as the cathode was adopted. Prior to the spin coating of ZnO electron transport layers (ETL), the patterned ITO on glass substrates was cleaned by detergent, organic solvents, and UV/ozone treatment sequentially. As a starting material, zinc acetate dehydrate ($Zn(CH_3COO)_2 \cdot 2H_2O$) was dissolved in anhydrous ethanol to prepare 0.1 M Zn^{+2} sol with monoethanol amine (MEA) added as a stabilizer in 1 molar ratio with Zn^{+2} [18-22]. The solution of mixture was then stirred at 80 ^{o}C for 1 hour to become clear and homogeneous. With MEA stabilizer, the precursor solution could be preserved for months without white precipitate of zinc hydroxide. Amorphous zinc oxide-acetate species (continuous gels) on

ITO/glass substrates was performed by spin-coating at 3000 rpm for 40 sec and being dried on a 200 ^{o}C hot plate. Subsequently, dry gels were transformed to be nanocrystalline ZnO films by thermal annealing, leading to the transmittance of ZnO films exceeding 90% within the visible range (not shown). A Cs_2CO_3 film was then deposited on ZnO films by thermal evaporation through a shadow mask, followed by spin-coating a red-emitting CdSe/ZnS QD (Aldrich, quantum yield > 30%) layer. The Cs_2CO_3 buffer layer was annealed at 200 ^{o}C under ambient conditions for 20 min to become robust and stable in air. Accordingly, 4,4`-bis(carbazole-9-yl)biphenyl (CBP), MoO_3, and Au layers were evaporated at about 5×10^{-6} torr, because large energy barrier between the valence band edges of MoO_3 (5.3 eV) and QD's shell material-ZnS (7.4 eV) can be decreased by inserting a CBP HTL which has larger HOMO energy (6.0 eV) [23]. The thickness of CBP, MoO_3, and Au was 30, 10, and 50 nm, respectively. The pristine MoO_3 layer was amorphous with an electrical conductivity of 1.1×10^{-4} S/cm. Our device structure can be depicted as $ITO/ZnO/Cs_2CO_3/QD/CBP/MoO_3/Au$. The overlap of ITO cathode and Au anode defined active area of devices to be 1.15 mm^2.
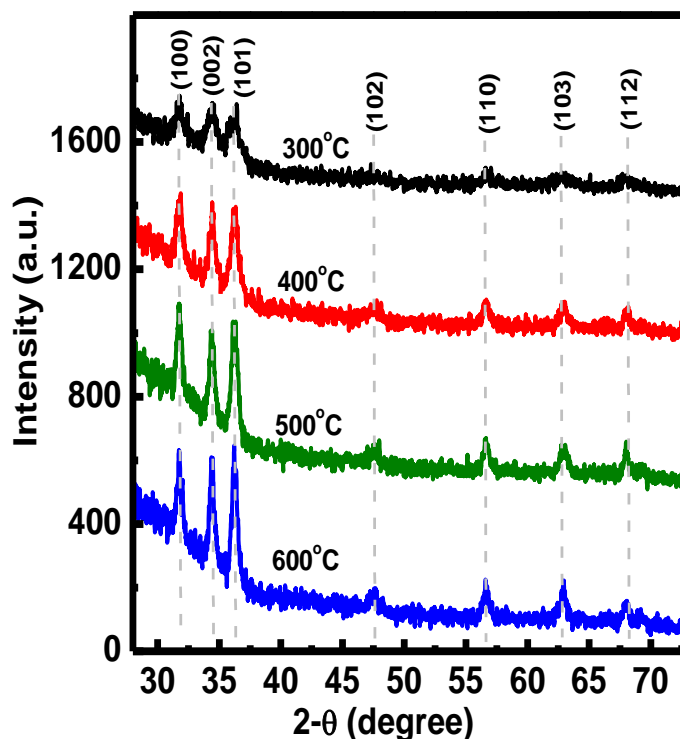
3. RESULTS AND DISCUSSION

Figure 1. X-ray diffraction patterns of nanocrystalline ZnO thin films annealed at 300, 400, 500, and 600 ^{o}C for 1 hour, respectively. Crystalline planes corresponding to all peaks are also indicated.

The crystallinity and crystal structure of sol-gel derived ZnO thin films were identified by x-ray diffraction (XRD) and scanning electron microscopy (SEM). As shown in Fig. 1, the XRD patterns of ZnO films annealed at different temperatures exhibit different degrees of crystallinity. These patterns

correspond to diffraction peaks of polycrystalline ZnO at (1 0 0), (0 0 2), (1 0 1), (1 0 2), (1 1 0), (1 0 3), and (1 1 2) planes (JCPDS 36-1451), which is apparently the hexagonal wurtzite structure [24]. The crystallinity is improved with increasing annealing temperature, despite that no obviously dominant peak was observed in all samples.
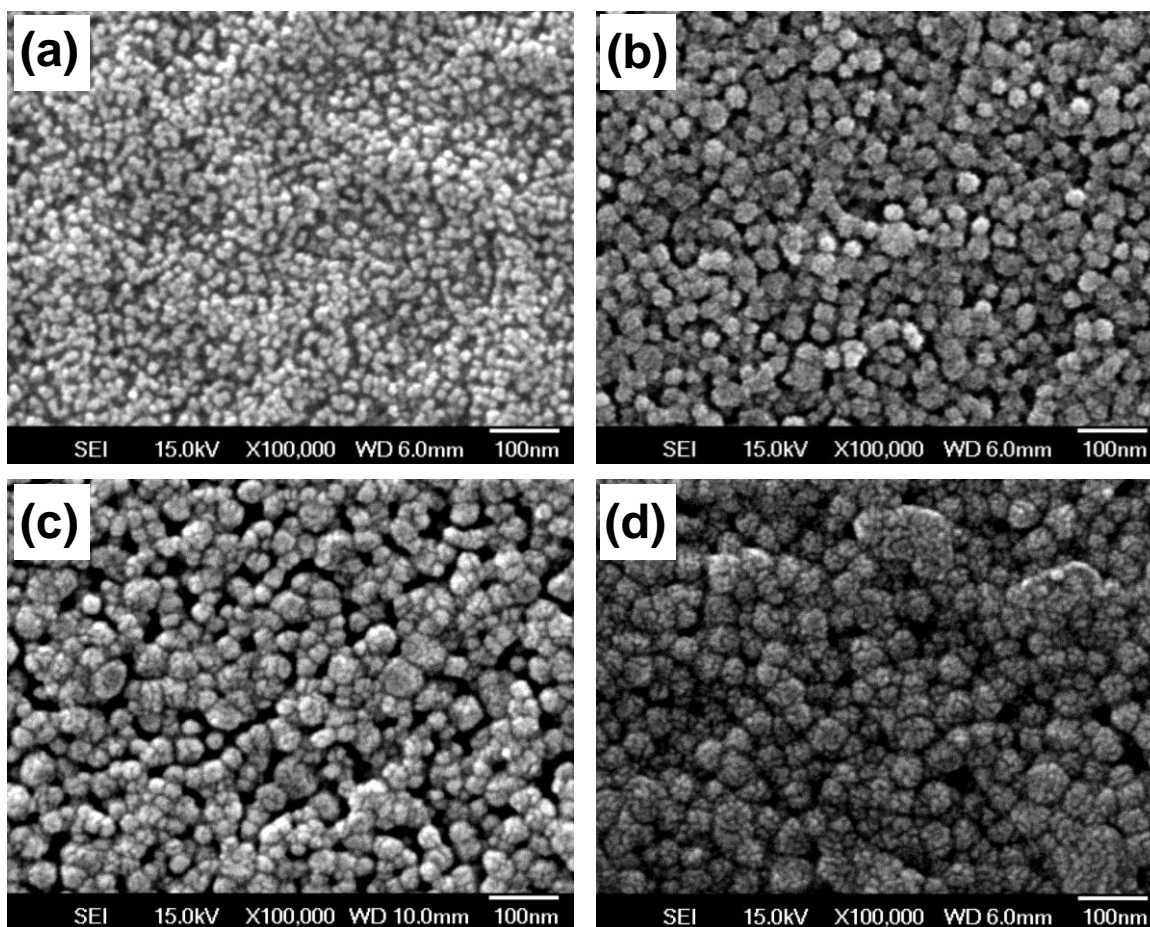

Figure 2. SEM images of ZnO thin films annealed at (a) 300, (b) 400, (c) 500, and (d) 600 $^{\circ}$C, respectively. The growth of crystal grains with annealing temperature was clearly observed. Scale bars represent 100 nm.

The SEM images of nanocrystalline ZnO films shown in Fig. 2 also exhibit the same trend. Large grain boundaries and dense nanopores are especially clear in samples annealed at higher temperatures; meanwhile the coalescence of adjacent grains becomes more pronounced for higher kinetic energy [18]. Besides the nanopores and grain boundaries, annealing at temperature above 400 $^{\circ}$C causes the degradation of conductivity and transmittance of beneath ITO. Therefore, only the ZnO films annealed at 400 $^{\circ}$C were used in the following device fabrication.

The current-voltage (*I-V*) and luminance-voltage (*L-V*) characteristics of fabricated QDLEDs with and without Cs_2CO_3 buffer layer were shown in Fig. 3. Without the Cs_2CO_3 layer to modify the surface morphology of ZnO thin films, the devices reveal a resistor-like instead of diode-like

characteristic that the magnitude of injection current is almost proportional to applied voltage. It is a strong sign of leakage current through unexpected leakage paths involved in device structure.
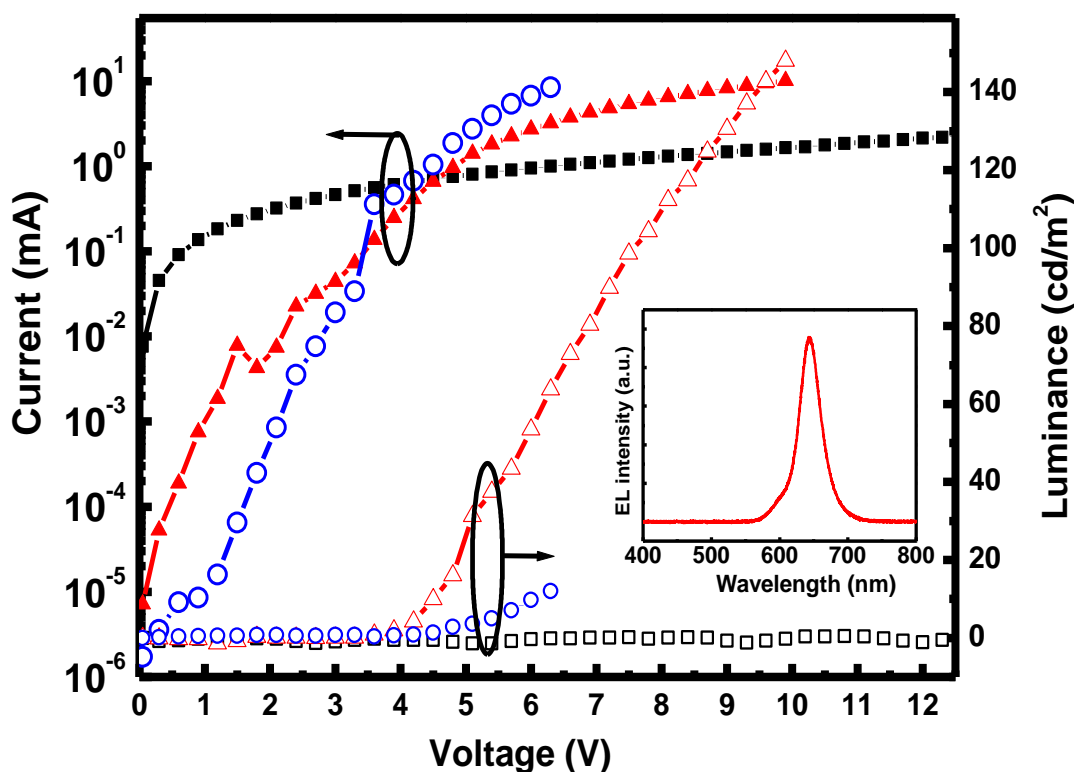

Figure 3. Current (full symbols) and luminance (open symbols) versus applied voltage for QDLEDs with (triangles and circles) and without (squares) Cs_2CO_3 buffer layer. Luminance of devices with annealed Cs_2CO_3 (triangles) is much larger than those with pristine Cs_2CO_3 (circles). Inset is EL spectra of devices with Cs_2CO_3 layer driven at 3 mA.

Consequently, there is no light emission from the devices over the whole operation range. On the contrary, the leakage current is significantly suppressed by inserting the Cs_2CO_3 buffer layer. When the devices with pristine (un-annealed) or annealed Cs_2CO_3 layer are compared, it is also definite that the modification of injection barrier is effective only after Cs_2CO_3 layer is annealed. As a result, the luminance turn-on voltage and maximum luminance efficiency is thus improved from 4.6 to 4.1 V and from 0.0017 to 0.026 cd/A, respectively. Inset of Fig. 3 shows the electroluminescence (EL) spectra of QDLEDs with annealed Cs_2CO_3 driven at 3 mA. The peak from QDs is located at 644 nm with a full width at half maximum (FWHM) of 35 nm. Most importantly, no light emission from CBP layer is observed.

To better understand the mechanism of Cs_2CO_3 buffer layer for suppressing leakage current, the surface morphology of pristine and annealed Cs_2CO_3 and subsequent QD layers was respectively examined by atomic force microscopy (AFM) (Model-NT MDT P47). As shown in Fig. 4(a), disordered microscale platelets are extensively distributed on the surface of pristine Cs_2CO_3 layer, leading to a large rms roughness of 7.8 nm. After annealing, the roughness is slight decreased to 6.1 nm and plenty of deep holes probably related to the pores or grain boundaries in ZnO are observed

(Fig. 4(b)). In Fig. 4(c), when the QD layer is coated on pristine Cs_2CO_3, crater-like structures appear and the surface is flattened to be with rms roughness of 2.6 nm.
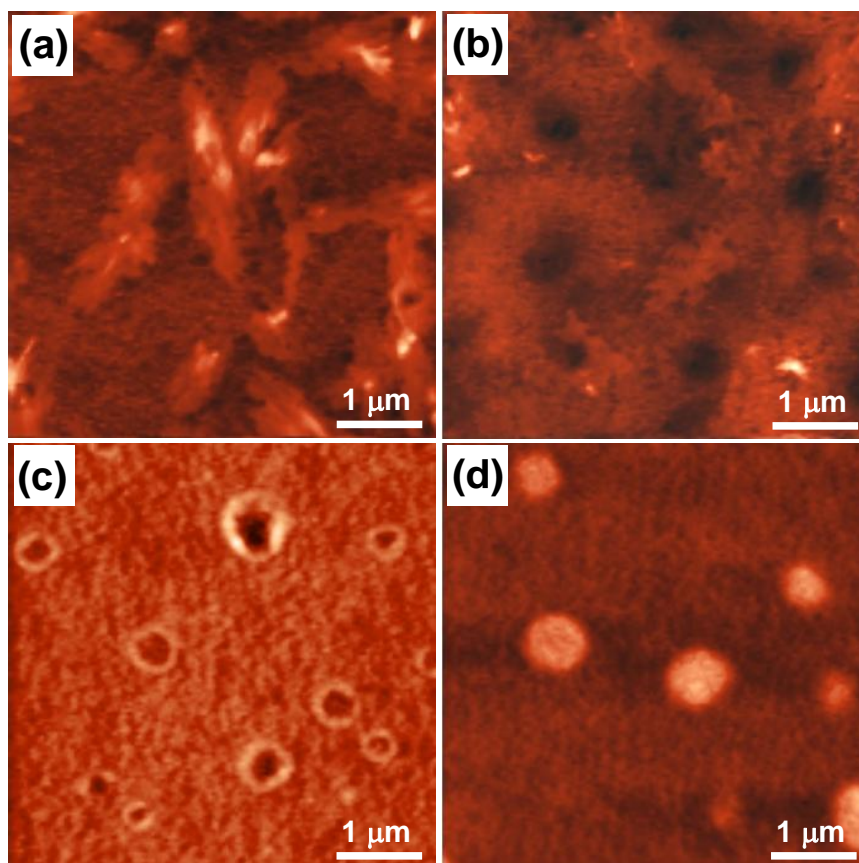

Figure 4. AFM images of (a) pristine and (b) annealed Cs_2CO_3 layers on ZnO ETL, on which QD layers (c)(d) exhibit distinct morphologies.

On the other hand, Fig. 4(d) shows that parts of QDs on annealed Cs_2CO_3 seem to aggregate and fill underneath holes, somehow those aggregated QDs evolve into distributed bumps with density smaller than that of holes in Cs_2CO_3. The rms roughness in Fig. 4(d) is about 5.1 nm. From these results, one can easily appreciate that large leakage current in devices without Cs_2CO_3 in Fig. 3 is essentially from the voids, nanopores and grain boundaries in ZnO films. Actually, the same phenomenon is frequently observed in ZnO varistors [25,26]. With the existence of these defects, QDs or CBP HTL may directly contact with ITO electrode. Once the Au electrode is forward applied, holes transported from CBP are conducted out through ITO electrode instead of being blocked by ZnO films. Though the leakage current can be greatly suppressed by inserting a Cs_2CO_3 layer, without annealing this buffer layer, the ZnO/QD interface is not effectively built-up for electron injecting. The unbalance of electrons and holes causes low luminance efficiency, obviously indicated by large difference between the turn-on voltages of current (~3.6 V) and luminance (~4.6 V) in Fig. 3. Finally, the aggregation and non-uniform distribution of QDs in Fig. 4(d) should be responsible for the fairly low luminance efficiency in devices with annealed Cs_2CO_3. Since the decrease of ETL surface roughness

results in a more even field distribution for uniform electron injection and Cs_2CO_3/QD typically inherit the surface features of underneath ETL, a flattened ZnO layer with minimized surface defects including voids, pores and grain boundaries should facilitate the improvement of device efficiency.

4. CONCLUSIONS

In conclusion, the effect of Cs_2CO_3 buffer layer in electroluminescent QDLEDs with ZnO and MoO_3 layers was experimentally demonstrated. Although the ZnO thin films were theoretically a good candidate for electron injection in QDLEDs, the sol-gel fabricated ZnO ETL might be porous and leakage paths could thus be formed without further treatment. We attributed the high current in devices without Cs_2CO_3 layer to the leakage of holes from CBP or QDs directly conducted to ITO electrode. The significant boost of performance of QDLEDs showed that the annealed Cs_2CO_3 buffer layer or related thin films with similar effects should be essential in the fabrication of QDLEDs.

References

1. X. Michalet, F. F. Pinaud, L. A. Bentolila, J. M. Tsay, S. Doose, J. J. Li, G. Sundaresan, A. M. Wu, S. S. Gambhir, and S. Weiss, *Science*, 307 (2005) 538.
2. Y. C. Chen, C. Y. Huang, H. C. Yu, and Y. K. Su, *J. Appl. Phys.*, 112 (2012) 034518.
3. C. Y. Huang, Y. K. Su, R. W. Chuang, and Y. C. Chen, *J. Electrochem. Soc.*, 156 (2009) H625.
4. Y. P. Hsieh, C. T. Liang, Y. F. Chen, C. W. Lai, and P. T. Chou, *Nanotechnol.*, 18 (2007) 415707.
5. C. Y. Huang, Y. K. Su, Y. C. Chen, P. C. Tsai, C. T. Wan, and W. L. Li, *IEEE Electron Dev. Lett.*, 29 (2008) 711.
6. H. Zhu, N. Song, H. Lv, C. L. Hill, and T. Lian, *J. Am. Chem. Soc.*, 134 (2012) 11701.
7. A. B. Greytak, P. M. Allen, W. Liu, J. Zhao, E. R.Young, Z. Popović, B. J. Walker, D. G. Nocera, and M. G. Bawendi, *Chem. Sci.*, 3 (2012) 2028.
8. C. Y. Huang, T. S. Huang, Y. C. Chen, C. Y. Cheng, C. T. Wan, M. V. M. Rao, Y. K. Su, *IEEE Photon. Tech. Lett.*, 22 (2010) 305.
9. L. Qian, Y. Zheng, J. Xue, and P. H. Holloway, *Nature Photon.*, 5 (2011) 543.
10. D. Kabra, L. P. Lu, M. H. Song, H. J. Snaith, and R. H. Friend, *Adv. Mater.*, 22 (2010) 3194.
11. Y. Wang, Q. Niu, C. Hu, W. Wang, M. He, Y. Zhang, S. Li, L. Zhao, X. Wang, J. Xu, Q. Zhu, and S. Chen, *Opt. Lett.*, 36 (2011) 1521.
12. N. Tokmoldin, N. Griffiths, D. D. C. Bradley, and S. A. Haque, *Adv. Mater.*, 21 (2009) 3475.
13. J. Shinar and R. Shinar, *J. Phys. D*, 41 (2008) 133001.
14. W. Hu, R. Henderson, Y. Zhang, G. You, L. Wei, Y. Bai, J. Wang and J. Xu, *Nanotechnol.*, 23 (2012) 375202.
15. S. Y. Ryu, B. H. Hwang, K. W. Park, H. S. Hwang, J. W. Sung, H. K. Baik, C. H. Lee, S. Y. Song, and J. Y. Lee, *Nanotechnol.*, 20 (2009) 065204.

16. C. Y. Huang, Y. K. Su, T. C. Wen, T. F. Guo, and M. L. Tu, *IEEE Photon. Technol. Lett.*, 20 (2008) 282.
17. A. Rizzo, Y. Li, S. Kudera, F. D. Sala, M. Zanella, W. J. Parak, R. Cingolani, L. Manna, and G. Gigli, *Appl. Phys. Lett.*, 90 (2007) 051106.
18. C. Y. Tsay, K. S. Fan, Y. W. Wang, C. J. Chang, Y. K. Tseng, C. K. Lin, *Ceram. Int.*, 36 (2010) 1791.
19. H. C. You and Y. H. Lin, *Int. J. Electrochem. Sci.*, 7 (2012) 9085.
20. C. Y. Huang, T. H. Wu, C. Y. Cheng, and Y. K. Su, *J. Nanopart. Res*., 14 (2012) 866.
21. H. Karami, *Int. J. Electrochem. Sci.,* 5 (2010) 720.
22. T. H. Wu, R. W. Chuang, C. Y. Huang, C. Y. Cheng, C. Y. Huang, Y. C. Lin and Y. K. Su, *Electrochem. Solid State Lett.*, 15 (2012) H208.
23. J. Kwak, W. K. Bae, D. Lee, I. Park, J. Lim, M. Park, H. Cho, H. Woo, D. Y. Yoon, K. Char, S. Lee, and C. Lee, *Nano Lett.*, 12 (2012) 2362.
24. D. Raoufi and T. Raoufi, *Appl. Surf. Sci.*, 255 (2009) 5812.
25. M. A. Ramirez, P. R. Bueno, W. C. Ribeiro, J. A. Varela, D. A. Bonett, J. M. Villa, M. A. Marquez, and C. R. Rojo, *J. Mater. Sci.*, 40 (2005) 5591.
26. M. A. Alim, S. Li, F. Liu, and P. Cheng, *Phys. Stat. Sol.*, 203 (2006) 410.